Second IEEE Conference on Control Applications, September 13 - 16, 1993 Vancouver, B.C.

Experimental Identification of Robot and Load Dynamic Parameters

Piotr Dutkiewicz Krzysztof R. Kozłowski Waldemar S. Wróblewski

Department of Control, Robotics and Computer Science
Technical University of Poznań
ul. Piotrowo 3a, 60-965 Poznań, Poland

Abstract — This paper presents an experimental identification of dynamic parameters of non-direct drive robot and load, which appear in the integral model, based on the energy theorem formulation. In the robotics literature, there are no experimental results known to the authors, concerning the identification of the integral model parameters. In order to satisfy this, an experimental set-up has been built around an industrial ASEA IRp-6 robot. Next, the robot dynamic integral model, taking into account friction parameters (viscous and Coulomb), as well as the load dynamic model have been formulated. The experimental results have been presented, including comparison of the results for both integral and differential identification.

I INTRODUCTION

Recently, robot control based on a mathematical model of the nonlinear and coupled arm and the gripped load dynamics reaches great importance. As the main purpose of it is the control with high speed and accuracy, the knowledge of the parameters of the dynamic model seems to be very significant. Therefore, many attempts have been carried out in identification of these parameters. Obviously, the simplest way is to take the robot to pieces, and then measure all the details thoroughly [2]. In most cases it is impossible, but when it is, it gives valuable benchmarks for other researchers. There are more practical methods, where the links of the robot are made to follow a predefined test trajectory [10, 12, 14, 1, 15]. The movement parameters (positions, velocities, etc.) are measured simultaneously, and from them the robot and load dynamic parameters can be calculated.

The experimental set-up has been built [8] around an industrial IRp-6 robot, built in Poland under the license of the Swedish ASEA. This is a typical non-direct drive industrial robot with five degrees of freedom, driven by DC motors, and with a 16-bit multiprocessor controller. The kinematic structure of the robot is presented in Fig. 1. Moreover, the robot is equipped with external measurement system enabling monitoring of each axis driving motor's position q_i, velocity $\dot{q}_i$, torque τ_i as well as with the force/torque sensors, mounted between the wrist of the manipulator and the gripper. During the experiments, the robot was equipped with one of following force/torque sensors: a German DLR and an American JR3.

The aim of this paper is to show the experimental identification of a non-direct drive robot and load dynamic parameters of the model derived using the energy theorem formulation (integral model). There are no experimental results of the identification of the integral model parameters available in the robotics literature, known to the authors. The integral model of robot dynamics, taking into account viscous and Coulomb friction parameters, as well as the load dynamic model have been formulated. In section II, the differential and integral dynamic models have been presented, including friction effects. In section III, the load dynamic integral model has been presented. In section IV, the identification algorithm, based on the least squares method and the Agee-Turner factorization, has been outlined. In section V, the experimental set-up has been depicted. In section VI, the experimental results of the integral robot and load model parameter identification have been presented. In section VII, some concluding remarks are presented.

II ROBOT DYNAMIC INTEGRAL MODEL

Consider a manipulator structure consisting of n rigid links, numbered in the increasing order from the fixed base (link 0) towards the tip (link n). Joint k connects links $(k-1)$ and k. The system contains only simple revolute and/or prismatic joints; each joint has one degree of freedom. Coordinate systems are assigned according to the modified Denavit-Hartenberg notation [6], but in general any other specific coordinate transformation can be used as well. The kinematic structure of the IRp-6 robot with coordinate frames assigned according to the modified

CH3243-3/93/0000-0767 $1.00 © 1993 IEEE

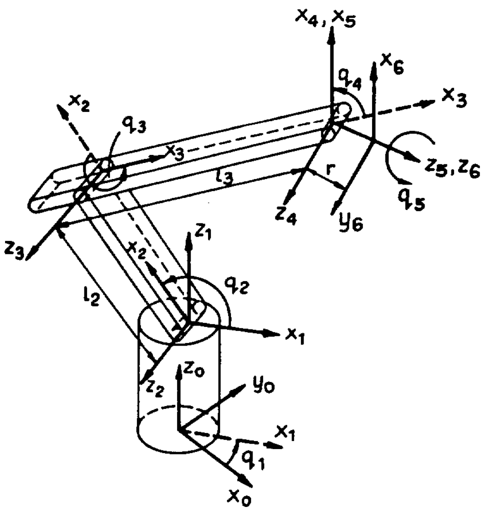

Figure 1: The kinematic structure of the IRp-6 robot

Denavit-Hartenberg notation is shown in Fig. 1.

The dynamic properties of the i-th link of the manipulator are characterized by the inertia tensor ${}^iI_i$, the first moment $m_i\,{}^ic_i$, and the mass m_i. The inertia tensor ${}^iI_i$ of the link i about the origin 0_i of the i-th coordinate system is the symmetric (3×3) matrix

$$ {}^iI_i = \begin{bmatrix} I_{ixx} & I_{ixy} & I_{ixz} \\ I_{ixy} & I_{iyy} & I_{iyz} \\ I_{ixz} & I_{iyz} & I_{izz} \end{bmatrix} . \tag{1} $$

The first moment $m_i\,{}^ic_i$ of link i, about the origin 0_i, is as follows

$$ m_i\,{}^ic_i = [m_i\,{}^ic_{ix},\ m_i\,{}^ic_{iy},\ m_i\,{}^ic_{iz}]^T , \tag{2} $$

where ${}^ic_{ix}$, ${}^ic_{iy}$, ${}^ic_{iz}$ are the coordinates of the center of mass of link i, expressed in the i-th coordinate frame, and $(\cdot)^T$ denotes the transpose operation.

The inertial parameters of the manipulator can be expressed by the $(10n \times 1)$ vector X'

$$ \begin{aligned} X' \ = \ & [I_{1xx}, I_{1xy}, I_{1xz}, I_{1yy}, I_{1yz}, I_{1zz}, m_1, m_1c_{1x}, \\ & m_1c_{1y}, m_1c_{1z}, \cdots, I_{nxx}, I_{nxy}, I_{nxz}, I_{nyy}, I_{nyz}, \\ & I_{nzz}, m_n, m_nc_{nx}, m_nc_{ny}, m_nc_{nz}]^T , \end{aligned} $$

and friction parameters by the $(2n \times 1)$ vector $X'' = [F_{1v}, F_{1s}, \cdots, F_{nv}, F_{ns}]^T$, where F_{iv} is the viscous friction coefficient of the i-th link, F_{ic} is the coefficient of the Coulomb friction (independent of the magnitude of the velocity). The friction generalized force acting at the i-th joint is assumed to be of the form

$$ Q_i(\dot{q}_i) = F_{iv}\dot{q}_i + F_{ic}\mathrm{sgn}(\dot{q}_i) , \tag{3} $$

where sgn$(\cdot)$ denotes the sign function. Inertial and friction parameters can be represented together as the vector X $(12n \times 1)$

$$ X^T = [X'^T,\ X''^T] . \tag{4} $$

Since the total energy of the robot is linear in these parameters [9, 11], the following vector equation can be written

$$ \tau = D(q, \dot{q}, \ddot{q})\ X , \tag{5} $$

where $q = [q_1, q_2, \cdots, q_n]^T$ is the vector of generalized coordinates q_i (angular or linear displacements), $\dot{q} = [\dot{q}_1, \dot{q}_2, \cdots, \dot{q}_n]^T$, $\ddot{q} = [\ddot{q}_1, \ddot{q}_2, \cdots, \ddot{q}_n]^T$, $\tau = [\tau_1, \tau_2, \cdots, \tau_n]^T$ is the vector of generalized forces τ_i (force or torque, depending on the type of the joint), and D is a $(n \times 12n)$ matrix, whose elements depend on q, $\dot{q}$, $\ddot{q}$. So described robot dynamic model is called a differential model.

The total kinetic and potential energy are linear in the parameters of the robot dynamic model [9, 11]. Thus we can write

$$ E_k = \sum_{i=1}^{M'} \frac{\partial E_k}{\partial X_i} X_i = \sum_{i=1}^{M'} DE_{ki}\ X_i , \tag{6} $$

$$ E_p = \sum_{i=1}^{M'} \frac{\partial E_p}{\partial X_i} X_i = \sum_{i=1}^{M'} DE_{pi}\ X_i , \tag{7} $$

where X_i is the i-th inertial parameter, $M' = 12n$ is the total number of inertial parameters of the manipulator, represented by the vector X'. DE_{ki} is a function of q, $\dot{q}$, and geometric parameters. DE_{pi} is a function of q and geometric parameters.

Making use of the energy theorem which states that the work of non-potential generalized forces applied to the system is equal to the change of the total energy of the system, it can be written that

$$ \begin{aligned} \int_{t_1}^{t_2} \tau^T \dot{q} dt \ &= \ (E_k(t_2) + E_p(t_2)) - (E_k(t_1) + E_p(t_1)) = \\ &= \ H(t_2) - H(t_1) , \end{aligned} \tag{8} $$

where τ is the vector of generalized non-potential forces, $E_k(t_i)$ and $E_p(t_i)$ are the kinetic and potential energy, respectively, of the manipulator at time instance t_i. $H(t_i) = E_k(t_i) + E_p(t_i)$ is the total energy of the system.

Assume, that τ_i is of the form

$$ \tau_i = \tau_{ei} - F_{ic}\ \mathrm{sgn}(\dot{q}_i) - F_{iv}\dot{q}_i , \tag{9} $$

where τ_{ei} is the generalized force exerted by the i-th actuator. The second term represents the generalized force vector of the Coulomb friction and the third term represents the generalized force vector of viscous friction. The friction coefficients are denoted as F_{ic} and F_{iv}.

As E_k and E_p are linear in the inertial parameters, comparing Eqs. (6) and (7) and taking into account Eq. (8) it can be written that

$$H(t_2) - H(t_1) = DL^T\ X' , \tag{10}$$

where

$$DL^T = [DL_1(t_2) - DL_1(t_1), \cdots, DL_M(t_2) - DL_M(t_1)] \tag{11}$$

and

$$DL_1(t_k) = DE_{ki}(t_k) + DE_{pi}(t_k) . \tag{12}$$

Define the friction coefficient vectors as

$$F_c = [F_{1c}, \cdots, F_{nc}]^T \tag{13}$$

and

$$F_v = [F_{1v}, \cdots, F_{nv}]^T . \tag{14}$$

In order to obtain a model that is linear in friction coefficients, introduce the following definitions

$$DF_c^T = \left[\int_{t_1}^{t_2} |\dot{q}_1| dt, \cdots, \int_{t_1}^{t_2} |\dot{q}_n| dt\right] \tag{15}$$

and

$$DF_v^T = \left[\int_{t_1}^{t_2} \dot{q}_1^2 dt, \cdots, \int_{t_1}^{t_2} \dot{q}_n^2 dt\right] . \tag{16}$$

Substituting Eqs. (13) and (14) in Eq. (8), the following equation is obtained:

$$y = \int_{t_1}^{t_2} \tau^T \dot{q} dt = DL^T\ X' + DF_s^T F_s + DF_v^T F_v . \tag{17}$$

X is the parameter vector ($12n \times 1$), $X^T = [X'^T,\ F_s^T,\ F_v^T]$, and $d^T = [DL^T, DF_s^T, DF_v^T]$. Then Eq. (17) can be rewritten in the following matrix form:

$$y = d^T\ X , \tag{18}$$

Eq. (18) represents a linear equation in the inertial and friction parameters, and vector d depends on q and $\dot{q}$. The model given by Eq. (18) does not require the knowledge of the joint acceleration. It is called the integral model [9] as opposite to the differential model (5).

III Load Dynamic Integral Model

The base coordinate frame $X_bY_bZ_b$ and the load of mass m are shown in Fig. 2. The origin of the local coordinate frame, in which forces and torques are measured, is denoted P. The point Q is situated at the center of mass of the load. Vectors from the base coordinate frame to the points P and Q are denoted p and q, respectively; c is the vector from P to Q. The equilibrium equations for the forces and torques acting at the load have the following form [4]:

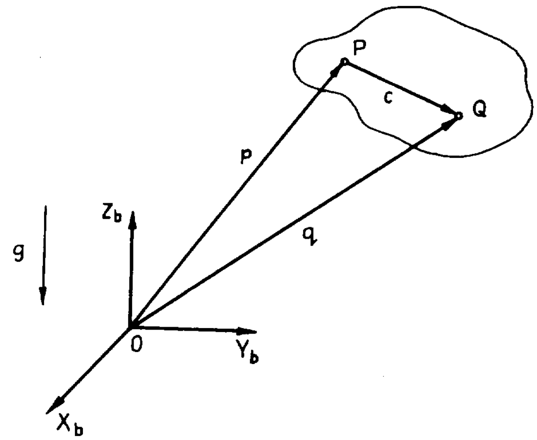

Figure 2: A rigid body in two different coordinate frames

$$\begin{aligned} F_q &= F + mg = m\ddot{q} , & (19)\\ N_q &= N - c \times F\ =\ I_q\, \dot{\omega} + \omega \times (I_q\, \omega) , & (20) \end{aligned}$$

where F and N are the force and torque vectors exerted by the sensor on the load at the point P; I_q is the inertia tensor with respect to the center of mass; g is the gravity vector; $\ddot{q}$ is the linear acceleration of the center of mass of the load; ω, $\dot{\omega}$ are the angular velocity and acceleration vectors. F_q and N_q are the resultant force and torque acting at the load of mass m, and '$\times$' denotes the cross product operation.

The accelerations of the vectors p and q are related by the formula [17]

$$\ddot{q} = \ddot{p} + \dot{\omega} \times c + \omega \times (\omega \times c) . \tag{21}$$

After substituting (21) in (19) and (20), the following equations are obtained:

$$\begin{aligned} F &= m\ddot{p} - mg + \dot{\omega} \times mc + \omega \times (\omega \times mc) , & (22)\\ N &= I_q\, \dot{\omega} + \omega \times (I_q\, \omega) + mc \times (\dot{\omega} \times c) + \\ &+ \ mc \times (\omega \times (\omega \times c)) + mc \times \ddot{p} - mc \times g . & (23) \end{aligned}$$

Assuming that the coordinate frames located at the points P and Q are parallel to each other, the inertia tensor about P can be calculated making use of Steiner's theorem [17]:

$$I_p = I_q + m\left[(c^T\ c)\mathcal{I} - (c\ c^T)\right] , \tag{24}$$

where $\mathcal{I}$ is the identity matrix.

Transforming double and triple cross products in (23) and using (24) leads to the following formula:

$$N = I_p\,\dot\omega + \omega \times (I_p\,\omega) + mc \times \ddot p - mc \times g\ . \qquad (25)$$

Equations (22) and (25) are linear in the dynamic parameters, i.e. the mass m, the static moment mc and the inertia tensor I_p. It is very important for the identification of these parameters.

To get a more compact form of (22) and (25), let us introduce the following notation:

$$\omega \times c = \begin{bmatrix} 0 & -\omega_z & \omega_y \\ \omega_z & 0 & -\omega_x \\ -\omega_y & \omega_x & 0 \end{bmatrix} \begin{bmatrix} c_x \\ c_y \\ c_z \end{bmatrix} \stackrel{def}{=} [\omega\times]c\ , \qquad (26)$$

and

$$I\omega = \begin{bmatrix} \omega_x & \omega_y & \omega_z & 0 & 0 & 0 \\ 0 & \omega_x & 0 & \omega_y & \omega_z & 0 \\ 0 & 0 & \omega_x & 0 & \omega_y & \omega_z \end{bmatrix} \begin{bmatrix} I_{xx} \\ I_{xy} \\ I_{xz} \\ I_{yy} \\ I_{yz} \\ I_{zz} \end{bmatrix} \stackrel{def}{=}$$

$$\stackrel{def}{=} [\,\cdot\,\omega]\begin{bmatrix} I_{xx} & I_{xy} & I_{xz} & I_{yy} & I_{yz} & I_{zz} \end{bmatrix}^T , \qquad (27)$$

where I_{ij} are elements of the inertia tensor I, ω_x, ω_y, ω_z are coordinates of the vector ω and c_x, c_y, c_z are coordinates of the vector c.

Taking into account this notation, (22) and (25) can be rewritten in the following form, often called the differential model:

$$W = K\,\Phi\ , \qquad (28)$$

where

$$W = \begin{bmatrix} F_x & F_y & F_z & N_x & N_y & N_z \end{bmatrix}^T$$

is a (6×1) vector consisting of force and torque coordinates, expressed in the local coordinate frame of the force/torque sensor. K is a (6×10) matrix of the following form:

$$K = \begin{bmatrix} \ddot p - {}^P_0R\,g & [\dot\omega\times] + [\omega\times][\omega\times] & 0 \\ 0 & [({}^P_0R\,g - \ddot p)\times] & [\,\cdot\,\dot\omega] + [\omega\times][\,\cdot\,\omega] \end{bmatrix}$$

depending on the load configuration in the base coordinate frame, i.e. on the changes of the vectors $\ddot p$, ω, and $\dot\omega$. Φ is a (10×1) vector of the load dynamic parameters,

$$\Phi = \begin{bmatrix} m & mc_x & mc_y & mc_z & I_{xx} & I_{xy} & I_{xz} & I_{yy} & I_{yz} & I_{zz} \end{bmatrix}^T ,$$

where mc_x, mc_y, mc_z are the static moment coordinates. All the parameters are expressed in the local coordinate frame with the origin located at the point P. Moreover, $g = [0, 0, g_0]^T$ is the gravity vector expressed in the base coordinate frame, and ${}^P_0R$ is the rotation matrix transforming the base coordinate frame to the local coordinate frame with the origin at the point P.

The acceleration signals $\ddot p$ and $\dot\omega$ occurring in (28), are difficult to measure. To avoid this, (28) can be integrated in the time interval $(t, t+T)$, in the local coordinate frame with the origin at the point P, affixed to the force/torque sensor. In this case the following integral model is obtained [7]:

$$\begin{bmatrix} \int_t^{t+T} F dt \\ \int_t^{t+T} N dt \end{bmatrix} = \left[\int_t^{t+T} K dt\right]\Phi = K_I\Phi\ , \qquad (29)$$

since the vector Φ does not depend on time. The first three rows of the matrix K_I are as follows:

$$\Big[v\,|_t^{t+T} + \int_t^{t+T} \omega \times v\, dt - \int_t^{t+T} {}^P_0R\, dt\ \ g,$$

$$[(\omega\,|_t^{t+T}\times] + \int_t^{t+T} [\omega\times][\omega\times]\, dt,\ 0 \Big]\ , \qquad (30)$$

and the next three rows are

$$\Big[0,\ [(-v\,|_t^{t+T} - \int_t^{t+T} \omega \times v\, dt + \int_t^{t+T} {}^P_0R\, dt\ \ g)\times],$$

$$[(\,\cdot\,\omega\,|_t^{t+T}] + \int_t^{t+T} [\omega\times][\,\cdot\,\omega]\, dt \Big]\ . \qquad (31)$$

These equations result from the basic relations describing the vectors and their derivatives in different coordinate frames [17]. Notice that linear and angular accelerations do not occur in (30) and (31). The linear velocity v and angular ω are expressed in the local coordinate frame. Like the differential model, the integral model is linear in the elements of the vector Φ.

IV Identification Scheme

The identification scheme for both robot and load dynamic models is the same. It is also the same for integral and differential models. Therefore, only the robot dynamic parameters identification algorithm for the integral robot dynamic model will be outlined. Moreover, it will be assumed that the model described by Eq. (18) is canonical, i.e. it is represented by the minimal set of the inertial parameters, which are the results of the regrouping (categorization) procedure. The least squares method in recursive form [5] will be used as the identification method.

The integral model is given by Eq. (18) and the goal is to find an estimate for the parameter vector X. In order to identify X, a sufficient number of equations, obtained by calculating the Eq. (18) in different time intervals, should be used. For the k-th interval $(t_1, t_2)_k$, such an equation has the form

$$y_k = d_k^T X , \tag{32}$$

where

$$d_k^T = [DL_k^T, DF_{ks}^T, DF_{kv}^T] . \tag{33}$$

Recall that y_k in Eq. (32) is the integral value of the dot product of generalized forces vector τ and generalized velocities vector $\dot{q}$ in time interval $(t_1, t_2)_k$, resulting from the work done by non-potential forces acting on the system. Assuming that k varies from 1 to r and taking into account Eq. (32), the following equation can be written:

$$y_r = h_r X + w , \tag{34}$$

where w is the observation error vector, $h_r = [d_1, \cdots, d_r]^T$, and $y_r = [y_1, \cdots, y_r]^T$. Assuming that $r > M_c$ (M_c is the number of inertial parameters of the canonical model, in general $M_c \neq 12n$), the least squares method leads to the formula

$$X = \left(h_r^T h_r\right)^{-1} h_r^T y_r . \tag{35}$$

The condition for the solution of this equation to exist is that matrix h_r be positive definite. Recursive solution of Eq. (35) has the following form [5, 10, 13, 14]:

$$X_{L+1} = X_L + P_{L+1} d_L (y_L - d_L^T X_L) , \tag{36}$$

$$P_{L+1} = P_L - (1 + d_L^T P_L d_L)^{-1} P_L d_L d_L^T P_L , \tag{37}$$

where $P_L = (h_L^T h_L)^{-1}$. With the solution known for L equations, the next step solution can be obtained using y_L and d_L, calculated in the time interval $(t_1, t_2)_L$. A common choice of the initial values in these equation is $P_0 = cI$ and $X_0 = 0$, where c is a constant and I is the identity matrix. In order to get positive definiteness of the P_L matrix during recurrences, the Agee and Turner factorization [5] has been used. Matrix P_L is presented in the form $P_L = U_L V_L U_L^T$, where U_L is an upper-triangular matrix with unit diagonal elements and V_L is a diagonal matrix. This approach leads to a numerically stable algorithm.

The proper choice of the testing signal is difficult. Armstrong [3] described the formal method in the general case. As this is not the subject of this paper, only the condition of persistent exciting will be quoted:

$$\forall\, \alpha, \beta \ \exists\, l : \alpha I < \sum_{k=l}^{l+\rho} P_{k+1} d_k d_k^T < \beta I , \ \ \rho > n \tag{38}$$

where ρ is the number of d functions. It appears that α should be sufficiently large. Testing the condition (38) for a trajectory class is a difficult optimizing task.

In the stochastic case, the signals q, $\dot{q}$, and τ are noisy, so one can write $\tilde{q} = q + v_p$, $\tilde{\dot{q}} = \dot{q} + v_s$, and $\tilde{\tau} = \tau + v_t$, where v_p, v_s and v_t are zero mean white processes. Similarly, the matrix d in Eq. (18) has the form $\tilde{d} = d(\tilde{q}, \tilde{\dot{q}})$. Eq. (18) can be rewritten

$$y = d^T X + v_m \tag{39}$$

where v_m represents a noise due to modeling error. Integrating $\tilde{\tau}^T \tilde{\dot{q}}$ leads to the following dependencies:

$$\tilde{y} = \int_{t_1}^{t_2} \tilde{\tau}^T \tilde{\dot{q}} dt = y + v_i . \tag{40}$$

Substituting (39) in Eq. (40), we obtain

$$\tilde{y} = \tilde{d}^T X + v_e , \tag{41}$$

where

$$v_e = d^T X - \tilde{d}^T X + v_m + v_i . \tag{42}$$

Notice that v_e is a random variable depending on v_p, v_s, v_m, and v_i, its explicit form being unknown. Moreover, v_e is correlated with vector d_k. Analogously to Eq. (34) one can write

$$y_r = h_r X + w . \tag{43}$$

In the last equation, y_r and w can be considered as realizations of random vectors Y_r and W, while h_r is a realization of a random matrix H_r. The matrices H_r are W correlated due to nonlinearities in H_r. Because H_r is a non-deterministic matrix and its explicit form is not known, it is not possible to use the Markov estimator. The effectiveness of vector X estimation can be determined using the least squares method. The estimator $\tilde{X}$ of X, whose realization is denoted as χ_r, is

$$\chi_r = \min_X \left[(y_r - h_r X)^T (y_r - h_r X)\right] . \tag{44}$$

The estimator given by Eq. (44) is biased because of the dependency of W and H_r. The estimator bias is equal to

$$E(X - \tilde{X}) = E\left[(H_r^T H_r)^{-1} H_r^T W\right] , \tag{45}$$

Fig. 3 shows the block diagram of the identification algorithm based on robot dynamic mathematical model and the robot itself.

For the k-th Eq. (18) different lengths of the time interval $(t_1, t_2)_k$ may be assumed. In case when $t_1 = t_0$ and $t_2 = t_k$, the observation of Eq. (18) is performed from the start with growing time interval. It is called a "long integral", as opposed to the "short integral" in the case when $t_1 \neq t_0$ or $t_2 \neq t_n$.

V Experimental Set-up

The block diagram of the experimental set-up [7, 8] is shown in Fig. 4. The main part of it is an IRp-6 robot, built in Poland under the license of the Swedish ASEA.

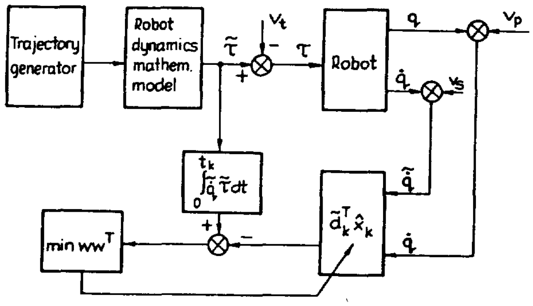

Figure 3: Identification of robot model parameters

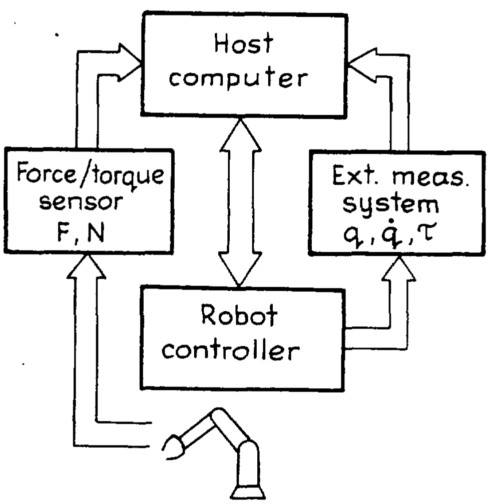

Figure 4: The block diagram of the experimental set-up

This is a typical industrial robot with five degrees of freedom, driven by DC motors. This robot has a parallelogram kinematic structure. The kinematic structure of the IRp-6 robot with coordinate frames according to the modified Denavit-Hartenberg notation is shown in Fig. 1.

The industrial robot controller is based on a 16-bit microprocessor, while each of the motors is controlled by a 8-bit microprocessor card. In order to have a fast and direct access to the robot controller hardware, a parallel 16-bit interface between a PC/AT-486 host computer and the robot controller has been used. Each motor's position, velocity, and current can be measured by means of a resolver, a tachometer, and the external measurement unit, enabling monitoring (with a sampling rate of 0.5 ms) of axis positions q_i, velocities $\dot{q}_i$, and currents of the DC motors of the robot, which are proportional to the driving torques τ_i.

A strain gauge force/torque sensor is used to measure, in the local coordinate frame, coordinates of force and torque exerted at the load gripped by the robot. The sensor is mounted between the wrist of the manipulator and the gripper. During the experiments, the robot was equipped with one of following force/torque sensors: a German DLR and an American JR3. The sampling frequency of the DLR and JR3 sensors are 30 Hz and 250 Hz, respectively. The possibilities of the DLR sensor, which is a prototype device, appeared to be rather poor comparing with the JR3 sensor. The latter is especially appropriate for industrial applications due to its accuracy and noise resistance.

VI Experimental Results

A. *Robot Parameters Identification*

The experimental identification of the IRp-6 robot inertial and friction parameters has been carried out for the first three links. The prerequisites of successful identification are the canonical model and trajectories fulfilling the persistent exciting condition. The parameterization of the IRp-6 robot dynamic integral model leads to 13 aggregated parameters $X_1, \cdots, X_{13}$ and accompanying expressions d (see Eq. (17)). For example:

parameter	d
$X_1 = I_{1zz} + I_{a1}n_1^2 + I_{2xx} + I_{3yy}$	$\frac{1}{2}\dot{q}_1^2$
$X_2 = I_{2yy} - I_{2xx} + m_3 l_2^2 - I_{3yy} + I_{3xx}$	$\frac{1}{2}\dot{q}_1^2 \sin^2 q_2$
$X_{10} = F_{3s}$	$\int \lvert\dot{q}_2 + \dot{q}_3\rvert dt$
$X_{13} = F_{3v}$	$\int (\dot{q}_2 + \dot{q}_3)^2 dt$

where elements of the form I_{ixx} are appropriate inertia tensor elements of the i-th link, I_{a1} is the actuator inertia moment of the first link, and n_1 is the gear ratio of the first actuator. Identification of all 13 parameters during simultaneous movement of the three links, using both short and long integral, did not complete successfully. Only 10 parameters were properly identified; for other parameters the d expressions appeared to be strongly linearly dependent. This is caused by the parallelogram structure of the manipulator.

Because of this, only movements of single joints as well as simultaneous movement of two joints were executed. During the movement of the 1-st joint 3 aggregated parameters can be obtained, during the movement of the 2-nd joint 4 parameters and during the movement of the 3-rd joint also 4 parameters can be obtained. Simultaneous movement of the 1-st and 3-rd joints allows identifying of 8 aggregated parameters. For example, the data measured during the movement of the 2-nd link allow to obtain the following aggregated parameters and the d expressions:

parameter	d
$X_1 = m_2 c_{2x} + m_3 l_2,$	$g\cos q_2,$
$X_2 = I_{2zz} + \left(\frac{dF_2}{d\phi_2}\right)^2 I_{a2} + m_3 l_2^2,$	$\frac{1}{2}\dot{q}_2^2,$
$X_3 = F_{2v},$	$\int \dot{q}_2^2 dt,$
$X_4 = F_{2c},$	$\int \lvert\dot{q}_2\rvert dt.$

where $\frac{dF_2}{d\phi_2}$ is a nonlinear function describing the gear ratio of the 2-nd link actuator.

The results of three separate movements of different single joints allow to identify all of the 13 aggregated parameters mentioned above. The X_2 parameter has been neglected as it is relatively small and difficult to identify. This procedure is fully reasoned when parameters are not easy to identify, e.g. it was also done by Seeger in [16].

As an example, identification results for the 2-nd link are presented. In Fig. 5 the test trajectory q_2, its velocity $\dot{q}_2$, torque τ_2, and energy plots are shown. The energy calculated using (18) is drawn with the solid line as opposed to the energy calculated using parameters and d_k (32), drawn with the dotted line. The test trajectory consists of splined polynomials of the 5-th order. The estimates $\hat{X}_1$, $\hat{X}_2$, $\hat{X}_3$, and $\hat{X}_4$ of the aggregated parameters are shown in Fig. 6. They are equal to $\hat{X}_1 = 8.125$ kgm (Fig. 6a), $\hat{X}_2 = 5.5$ kgm^2 (Fig. 6b), and the friction parameters $\hat{X}_3 = 26$ Nms (Fig. 6c), and $\hat{X}_4 = 28.75$ Nm (Fig. 6d). The estimates, calculated using (36), settle in the time of 1.0 to 1.5 s and 8000 samples have been measured for one movement.

The presented results were calculated using short integral (with the step of 5 ms). The results of long integral were significantly worse, as in this case the errors of the measurements of $\dot{q}$ and τ were accumulated. This effect was also noticed by An et al. in [1].

B. Load Parameters Identification

All the parameters were estimated using the JR3 sensor because of the reasons mentioned in section IV. The least squares method in recursive form [5] with Agee and Turner factorization have been used for identification.

First, the differential model with dynamic parameters,

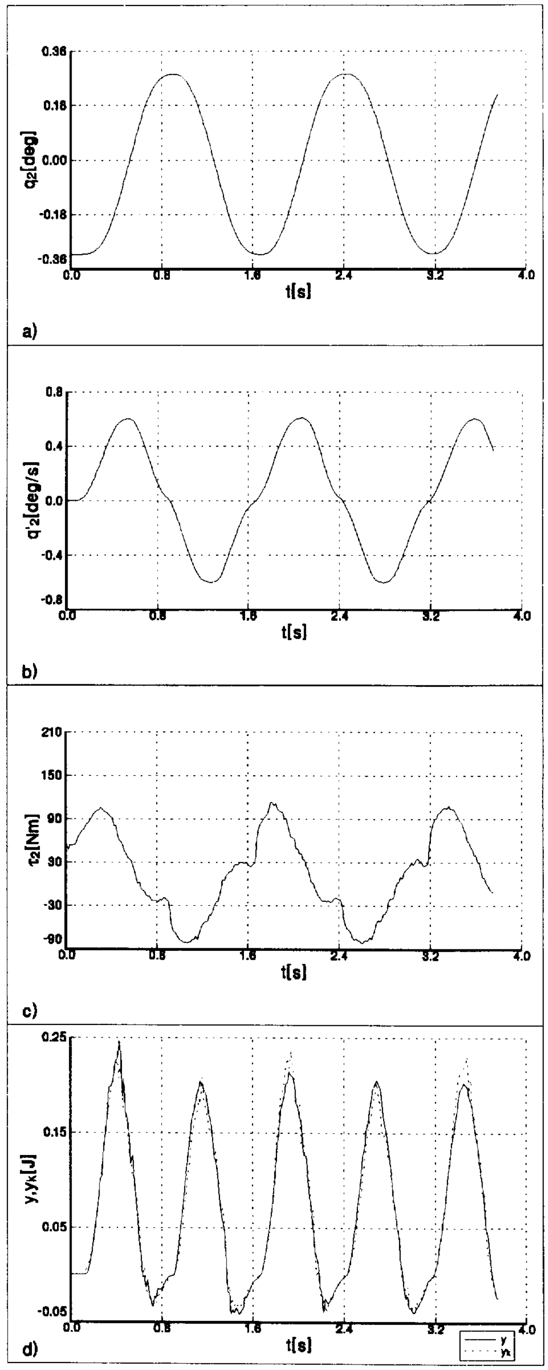

Figure 5: q_2, $\dot{q}_2$, τ_2, and energy as functions of time

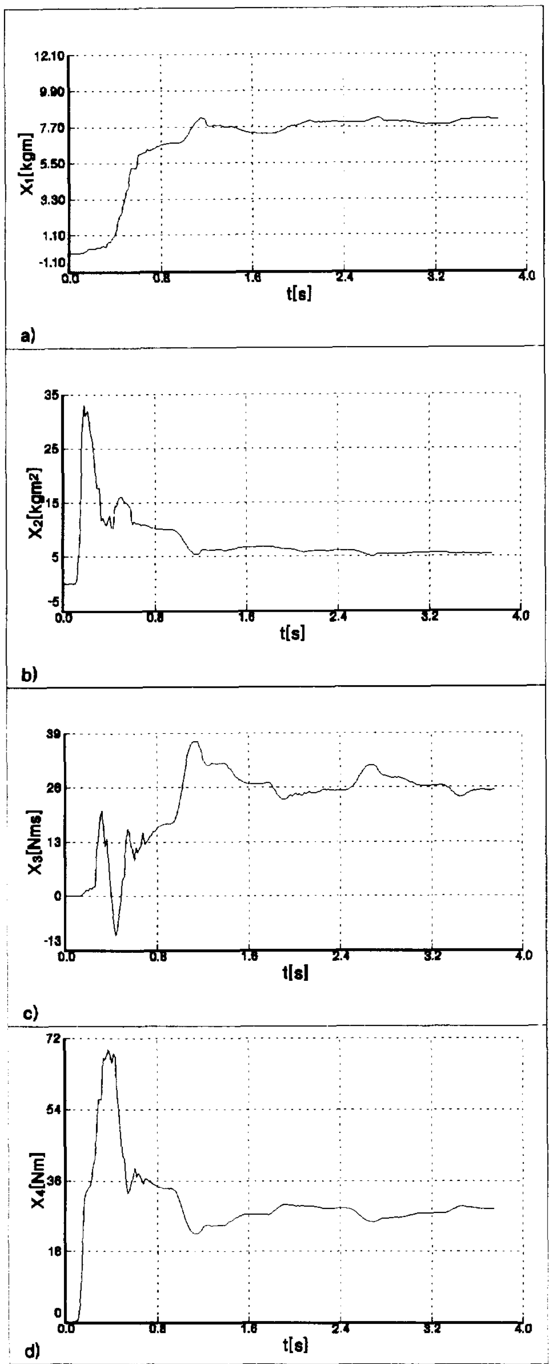

Figure 6: Estimates of robot parameters X_1, X_2, X_3, X_4

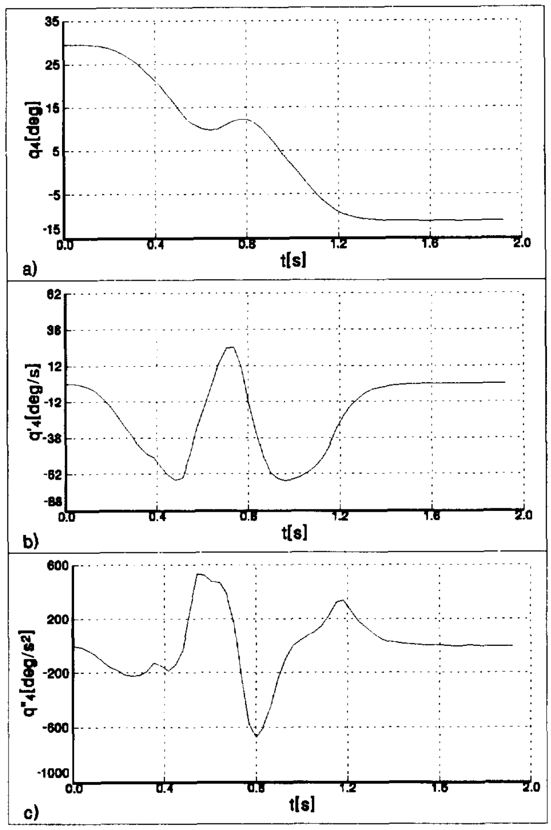

Figure 7: q_4, $\dot{q}_4$, $\ddot{q}_4$ as functions of time

TABLE I
DYNAMIC PARAMETERS OF THE LOAD

Parameter	Computed Values	Estimated Values
m $[kg]$	1.910	1.916
mc_x $[kgm]$	0.0573	0.0568
mc_y $[kgm]$	−0.0210	−0.0207
mc_z $[kgm]$	0.1394	0.1396
I_{xx} $[kgm^2]$	0.01050	0.01186
I_{xy} $[kgm^2]$	0.00094	−0.00083
I_{xz} $[kgm^2]$	−0.00450	−0.00751
I_{yy} $[kgm^2]$	0.01635	0.01567
I_{yz} $[kgm^2]$	0.00169	0.00001
I_{zz} $[kgm^2]$	0.00520	0.00449

described by Eq. (28), has been used [7]. As an example, the identification results of a steel cuboidal load are presented. Its dynamic parameters are easy to calculate using its measured mass and geometric parameters. Dynamic parameters, presented in Table I, were determined in the local coordinate frame, assigned to the force/torque sensor.

Since the velocity signals, measured using tachometers, are not sufficiently accurate, the position signals were numerically differentiated and compared to the velocity signals. They appeared to be more accurate, even for a simple 3-point differentiating filter, with a sample interval of $\Delta t = 32ms$. The acceleration signal was obtained by differentiating the velocity. It was assumed that the movement of each joint was described by a polynomial of the 5-th order in the joint coordinate. The ranges of the movement were as follows:

$$\begin{aligned} -40^\circ &\leq q_1 \leq 30^\circ , \\ 10^\circ &\geq q_2 \geq -20^\circ , \\ -30^\circ &\leq q_3 \leq 40^\circ , \\ 30^\circ &\geq q_4 \geq -10^\circ , \\ -150^\circ &\leq q_5 \leq -10^\circ . \end{aligned}$$

The time of the movement was equal 1.83 s for each joint. Example position (a), velocity (b), and acceleration (c) signals for the 4-th joint are shown in Fig. 7.

Fig. 8a shows the estimate of mass m and Fig. 8b presents the estimates of static moment coordinates mc_x, mc_y, mc_z. Estimates of inertia moments I_{xx}, I_{yy}, I_{zz} are shown in Fig. 8c, and estimates of inertia products I_{xy}, I_{xz}, I_{yz} in Fig. 8d. Comparing the estimates to the computed values (see Table I), it can be noticed that the mass and the static moment were estimated exactly. The estimates of the inertia products, smaller than the inertia moments, are worse, though the results do not differ significantly from the computed values. It is consistent with similar results presented in [1] and [4].

The movement of the robot arm during the identification measurements was the fastest possible. With slow movements, it was only possible to identify mass and static moment. It is obvious that it was impossible to identify the inertia tensor elements in such case. As the trajectories polynomials of the 3-rd and 5-th order have been used, both with good results.

Some problems have been met when using the integral model, described by Eq. (29). Generally, when both "short integrals" and "long integrals" were used, the parameter estimates were worse than those for differential model, and the set of scalar equations had tendencies to linear dependencies. As a consequence of integration, large errors coming from cumulated low-frequency measurement disturbances have been obtained. When only some of scalar

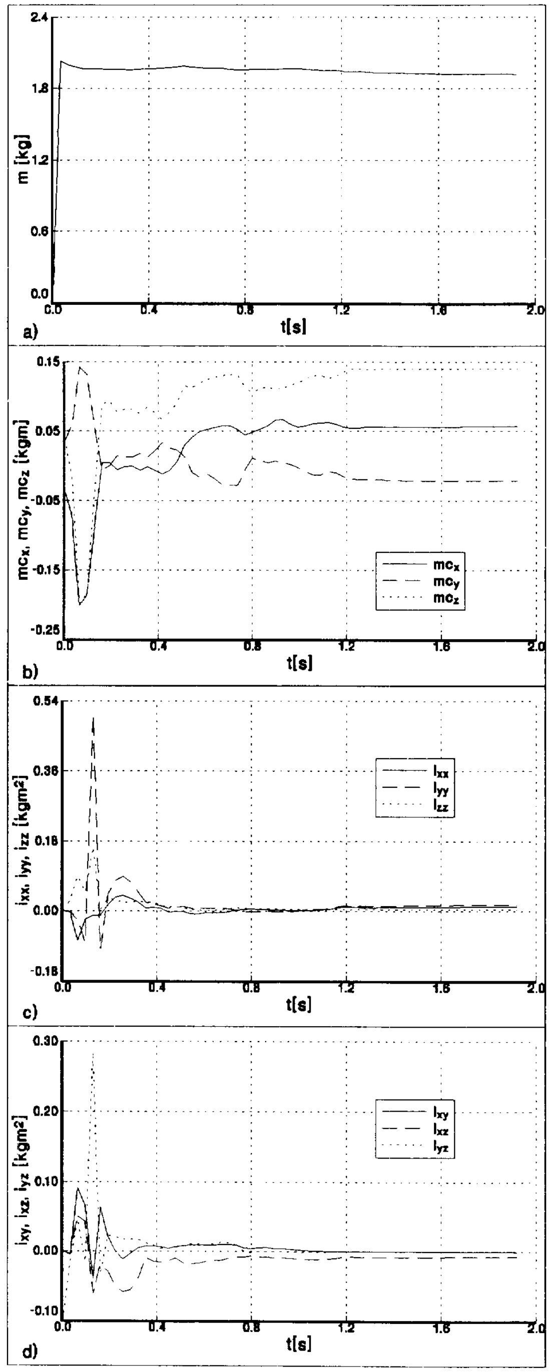

Figure 8: Estimates of load dynamic parameters

equation from vector Eq. (29) have been used, the results were significantly better.

VII Concluding Remarks

Though a relatively fast computer (PC AT/486 50, MHz) was used, the calculation of the parameters had to be executed off-line, after the data acquisition during the arm movement. Interesting seem attempts of on-line calculations of the parameters. They require optimizing the identification algorithm as well as upgrading the measurement and computational units.

Identification of inertial and friction parameters of the IRp-6 robot model as well as of inertial parameters of the loan model is a preliminary work. The dynamic model of the ASEA IRp-6 robot will be used for control based an the identified model, which is currently under investigation.

Acknowledgements

The research presented in this paper was supported by Grant No. 1096-S5-92-02 from KBN (Polish Committee on Scientific Research). K. R. Kozłowski and W. S. Wróblewski were also supported by Grant No. 92-2072 from the Foundation for Promotion of Advanced Technology, Japan.

References

[1] Ch.H. An, Ch.G. Atkeson, J.M. Hollerbach, *Model-Based Control of a Robot Manipulator*, The MIT Press, 1988.

[2] B. Armstrong, O. Khatib, J. Burdick, "The Explicit Dynamic Model and Inertial Parameters of the PUMA 560 ARM", in *Proceedings of the IEEE International Conference on SMC*, 1986, pp. 510-518.

[3] B. Armstrong-Hélouvry, *Control of Machines with Friction*, Kluwer Academic Publishers, 1991.

[4] Ch.G. Atkeson, Ch.H. An, J.M. Hollerbach, "Rigid Body Load Identification for Manipulators", in *Proceedings of the 24th Conference on Decision and Control*, Ft. Lauderdale, 1985, pp. 996-1002.

[5] G.J. Bierman, *Factorization Methods for Discrete Sequential Estimation*, Academic Press, New York, 1977.

[6] J.J. Craig, *Introduction to Robotics. Mechanics and Control*, Addison-Wesley Publishing Company, 1989.

[7] P. Dutkiewicz, K. Kozłowski, W. Wróblewski, "Experimental Identification of Load Parameters", in *Proceedings of the IEEE Int. Symp. on Industrial Electronics*, Budapest, 1993, pp. 361-366.

[8] P. Dutkiewicz, K. Kozłowski, W. Wróblewski, "Robot Programming System for Research Purposes", in *Proceedings of the COMPEURO'93*, Paris-Evry, 1993, pp. 94-101.

[9] M. Gautier, "Identification of Robot Dynamics", in *Proceedings of the IFAC/IFIP/ IMACS International Symposium on Theory of Robots*, Vienna, 1986, pp. 351-356.

[10] M. Gautier, W. Khalil, "On the Identification of the Inertial Parameters of Robots", in *Proceedings of the 27th CDC*, 1988, pp. 2264-2269.

[11] W. Khalil, J.F. Kleinfinger, "Minimum Operations and Minimum Parameters of the Dynamic Models of Tree Structure Robots", *IEEE Journal of Robotics and Automation*, Vol. RA-3, No. 6, pp. 517-526, 1987.

[12] P.K. Khosla, *Real-Time Control and Identification of Direct-Drive Manipulators*, Ph.D. Thesis, Department of Electrical and Computer Engineering, The Robotics Institute, Carnegie Mellon University, 1986.

[13] K. Kozłowski, "Identification of Model Parameters of Robotic Manipulators", *Systems Science*, Vol. 18, No. 1-2, pp. 165-187, 1992.

[14] K. Kozłowski, M. Prüfer, "Parameter Identification of an Experimental 2-Link Direct Drive Arm", in *Proceedings of the IASTED International Conference, Control and Robotics*, Vancouver, 1992, pp. 313-316.

[15] H.B. Olsen, G.A. Bekey, "Identification of Robot Dynamics", in *Proceedings of the IEEE Int. Conf. on Robotics and Automation*, San Francisco, 1986, pp. 1004-1010.

[16] S. Seeger, "Self-Tuning Control of a Commercial Manipulator Based on an Inverse Dynamic Model", in *Proceedings of the Symposium on Robot Control SYROCO'91*, Vienna, 1991, pp. 453-458.

[17] J. Wittenburg, *Dynamics of Systems of Rigid Bodies*, B.G. Teuber, Stuttgart, 1977.